Structural Analysis and Thermal Stability of Natural Magnetite (Fe_3O_4) from Nasasrawa state, Nigeria: Insights from XRD, FTIR, and Thermogravimetric Analysis

DAHIRU M.A[1], RIDWAN MUHAMMAD MAHMOOD[2], HAUWA M MARI[3], IBRAHIM GANA GEIDAM[4]

[1,3]Department of Physics, Federal College of Education (T) Potiskum Yobe State Nigeria

[2]Department of Applied Geophysics, Federal University Birnin Kebbi, Kebbi State Nigeria.

[4]Department of Physics, Yobe State University Damature Yobe State Nigeria.

Corresponding Author; mdabdulpot29@gmail.com, ORCID NUMBER: 0009-0007-2238-9191

ABSTRACT

In this study, the thermal behavior and structural characteristics of natural magnetite obtained from Nasarawa State, Nigeria, were investigated. The samples were heated at 250, 500, 750, and 1000 °C using a laboratory muffle furnace (C200 model) and subsequently characterized using X-ray diffraction (XRD), Fourier transform infrared spectroscopy (FTIR), and thermogravimetric analysis (TGA). XRD results showed that magnetite was the dominant mineral phase, with its characteristic (311) diffraction peak observed at $2\theta = 35.39°$, confirming a well-crystallized cubic spinel structure. Small amounts of quartz and orthoclase were also detected as naturally associated minerals. FTIR analysis revealed gradual changes in the Fe–O vibration bands with increasing temperature, indicating structural rearrangement during heating while preserving the fundamental crystal structure below 500 °C. The TGA results showed only slight mass loss below 700 °C, whereas more pronounced weight loss occurred at higher temperatures because of oxidation of magnetite to hematite and transformations of minor impurity phases and the stability was observed at approximately 567°C. Overall, the findings demonstrate that the Nigerian magnetite possesses good thermal stability and maintains its structural integrity over a broad temperature range. These properties support its potential use in high-temperature applications, including radiation shielding materials, refractory products, magnetic components, and catalyst supports.

Keywords: Magnetite; Thermal stability; XRD; FTIR; Thermogravimetric analysis; Radiation shielding.

1. Introduction

Magnetite is a naturally stirring iron oxide mineral with the chemical formula Fe_3O_4 (He et al., 2023; Reddy et al., 2023) and It is one of the key iron ores and has a characteristic black or brownish-black color and a metallic luster (Jeong 2024). Magnetite is famous for its magnetic properties; it is the most magnetic of all the naturally occurring minerals on Earth (Dudchenko et al., 2022; Fock et al., 2017). However, magnetite is a mixed iron (II) and (III) oxide in cubic inverse spinel structure. Large types of metals and molecules can be easily restrained and supported on the surface of magnetite. These properties of magnetite, make this solid support a good choice; it is a non-poisonous material and relatively inert (Abraham et al., 2021; Liu et al., 2023). These properties have made magnetite valuable in a wide range of industrial applications, including metallurgy, catalysis, wastewater treatment, magnetic devices, pigments, and, more recently, radiation shielding materials (Cornell & Schwertmann, 2003; Mahdavi et al., 2013; Morel et al., 2013).

Magnetite is used in many biomedical fields, including the treatment of hyperthermia, the isolation of genomic DNA, the process of surface functionalization, radiation shielding materials, the use of magnetite as composite iron oxide nanoparticles, the use of magnetite as magnetic materials in catalytic applications, optics (including nanophotonics, magnetic field sensors, and magnetic resonance imaging technology), the oil and gas industries, the environment, and other fields (Abdullah et al. 2022; Arakaki et al. 2008; Bustamante-Torres et al. 2022).

The performance of magnetite in these applications depends not only on its chemical composition but also on its ability to maintain its structural integrity when exposed to elevated temperatures. Thermal exposure may induce oxidation, structural rearrangement, and phase transformations that can alter its physical and functional properties (Cornell & Schwertmann, 2003; Oukafir et al., 2023). Understanding these thermal changes is particularly important for applications such as radiation shielding concrete, refractory materials, thermal energy storage systems, and metallurgical processing, where the material is expected to perform reliably under harsh thermal conditions (Duglet et al., 2025).

Several analytical techniques have been employed to investigate the structural and thermal behavior of magnetite. X-ray diffraction (XRD) is widely used to identify crystalline phases and evaluate structural modifications, Fourier transform infrared spectroscopy (FTIR) provides information on chemical bonding and functional groups, while thermogravimetric analysis (TGA) is an effective tool for monitoring mass-loss behavior, thermal decomposition, and phase transformations during heating (Murbe et al., 2008; Fawcett et al., 2022; Nandiyanto et al., 2023). The combination of these complementary techniques provides a comprehensive understanding of the thermal evolution and structural stability of magnetite.

Although the structural properties of synthetic magnetite and magnetite nanoparticles have been extensively reported, comparatively little information is available on the thermal behavior of naturally occurring Nigerian magnetite. Since natural magnetite commonly contains accessory minerals such as quartz and feldspars, its thermal response may differ from that of synthetic materials. Therefore, this study investigates the mineralogical composition, thermal stability, and temperature-induced structural changes of natural magnetite collected from Nasarawa State, Nigeria, using XRD, FTIR, and TGA. The findings contribute to the understanding of the thermal performance of Nigerian magnetite and provide valuable information for its potential application in radiation shielding and other high-temperature engineering systems.

2.0 Material and Method

2.1 Sample collection and preparation

The magnetite samples were collected from Nasarawa State, the north-central part of Nigeria, and then air-dried in the laboratory at room temperature (20–25°C) for 24–48 hours to remove the moisture content, and then the samples were cleared from stones and pebbles. The dried samples were preliminarily crushed, sieved to a particle size less than 0.5 mm, and mixed thoroughly to ensure homogeneity.

2.2 Sample thermal treatment

Magnetite (Fe_3O_4) powder samples were prepared and placed in alumina crucibles for thermal treatment. A laboratory muffle furnace Nabertherm (C200 model) was used to heat the samples under atmospheric conditions. The furnace was pre-heated to the target temperature before sample insertion to ensure accurate temperature exposure.

For each temperature, approximately 200g of magnetite powder was loaded into a clean alumina crucible and placed in the furnace chamber.

Samples were heated to four different target temperatures: from the room temperature 25°C to 250°C, 500 °C, 750 °C, and 1000 °C. The temperature was increased at a controlled ramp rate of 1°C/min. The corresponding ramp durations were approximately 225, 475, 675 and 975 minutes, respectively. Once the target temperature was achieved, the samples were held (isothermally) at that temperature for 2 hours to ensure thermal equilibration.

After the hold time, samples were removed from the furnace and allowed to cool to room temperature in ambient air inside the furnace. After cooling, the samples were stored in desiccators prior to further characterization.

2.3 X-ray diffraction (XRD) analysis of magnetite

The mineralogical composition and crystalline phases of the magnetite sample were characterized using a Rigaku MiniFlex 600-C X-ray diffractometer. Prior to analysis, the sample was crushed, pulverized into fine powder, sieved to a particle size of 45 μm, homogenized thoroughly, and stored in airtight containers following the sample preparation procedure described by García-Maté et al. (2025). XRD measurements were conducted using Ni-filtered Cu-Kα radiation (λ = 1.5406 Å) operated at 40 kV and 30 mA. Diffraction patterns were recorded over a 2θ range of 2°–70°, and phase identification was performed by comparison with the International Centre for Diffraction Data (ICDD) Powder Diffraction File (PDF) database (Fawcett et al., 2022).

The average crystallite size was estimated using the Debye–Scherrer equation (Debye and Scherrer, 1918):

$$D = \frac{K\lambda}{\beta_{\frac{1}{2}} \cos\theta} \qquad \ldots(1)$$

where D is the crystallite size, K is the shape factor (≈0.9), λ is the X-ray wavelength, β is the full width at half maximum (FWHM) of the diffraction peak in radians, and θ is the Bragg diffraction angle.

2.4 FTIR Sample Analysis

FTIR spectrum of the magnetite sample was obtained using Perkin Elmer-2, an advanced FTIR spectrophotometer at Ahmadu Bello University Zaria multi-user laboratory. After preliminary preparation, the samples were further ground to about 1-2 mg using an agate mortar and pestle to a fine powder in order to achieve sample homogeneity. The instrument emits a beam of infrared radiation that passes through the sample and a detector in the frequency ranged (4000-400 cm^{-1}) while recordings the amount of radiation transmitted by the sample at each frequency. This process produces a spectrum that represents the unique absorption pattern of the sample.

3.5 TGA thermal analysis

Thermogravimetry (TGA) was conducted using thermogravimetric analyzer (TGA 400 Perkin Elmer made in Netherlands).The calibration of the instrument; such as temperature, furnace and weight calibration was carried out according to manufacturer's recommendation. About 15mg of the magnetite sample was used to measure the significant transition temperature and transformation mechanisms of the magnetite sample. The sample was loaded onto a platinum sample pan. Constant heating and cooling scans were performed on barite powder samples, under a flux dry, from 30.00°C up to 1000°C with a heating and cooling rate of 10.00°C/min in air atmosphere.

3.0 Results and Discussion

3.1. XRD analysis of magnetite

Figure 1 presents the XRD pattern of the magnetite sample, while the corresponding diffraction data are summarized in Table 1. The diffraction peaks observed between 30.09° and 67.66° (2θ) confirm that magnetite (Fe_3O_4) is the dominant crystalline phase. The most intense reflection occurs at 2θ = 35.39°, corresponding to the (311) crystallographic plane, which is the characteristic diffraction peak of cubic spinel magnetite. The identified phase matches ICDD PDF Card No. 00-002-1035 with the Fd-3m (No. 227) space group, confirming the formation of highly crystalline magnetite.

Table 1. XRD analysis of magnetite sample

Phase name	Chemical formula	Miller indices (hkl)	2Θ°	FWHM°	Crystalline size(nm)
Magnetite	**Fe_3O_4**	**(311)**	**35.39**	**0.22**	**39.90**
Orthoclase	**$Al_2O_3 \cdot K_2$**	**(130)**	**22.80**	**0.30**	**27.00**

Quartz	**O ·6 Si O_2 Si O_2**	**(212)**	**53.19**	**0.55**	**16.60**

The calculated crystallite size of 39.90 nm indicates that the sample consists of nanocrystalline magnetite, which agrees well with the value of 38.7 nm reported by Morel et al. (2013). The prominent (311) reflection is widely recognized as the fingerprint peak of magnetite and confirms the preservation of its inverse spinel cubic crystal structure. Similar diffraction characteristics have been reported by Murbe et al. (2008) and Mahdavi et al. (2013), who associated the intense (311) peak with the high crystallinity and phase purity of magnetite.

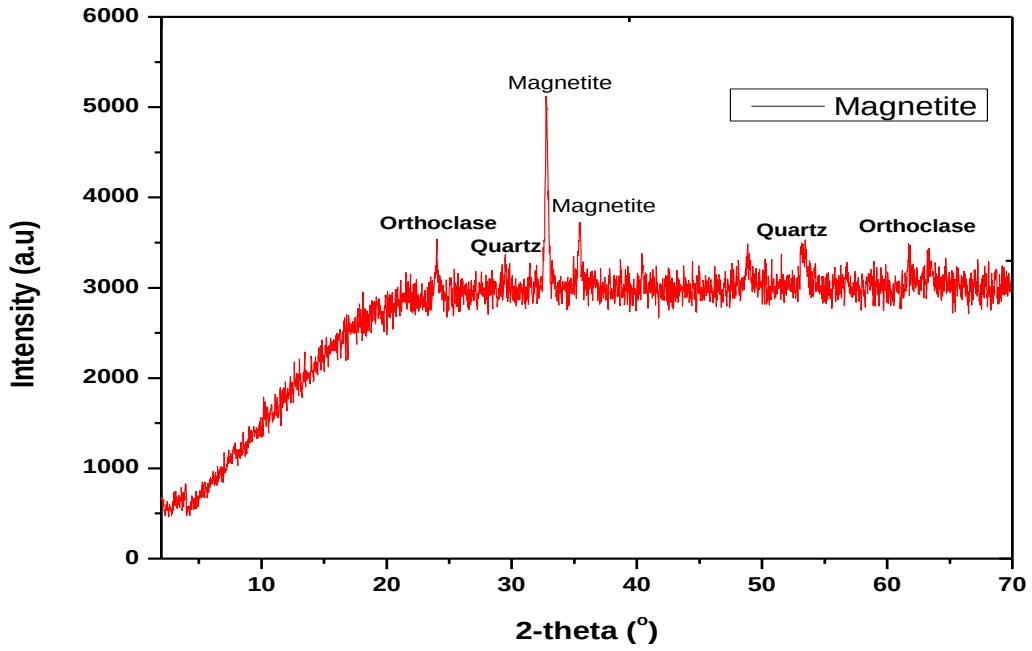

Figure 1: XRD patterns of the analyzed magnetite mineral

Besides magnetite, minor diffraction peaks corresponding to orthoclase $Al_2 O_3 \cdot K_2O \cdot 6 SiO_2$ and quartz (SiO_2) were identified. Orthoclase was detected at 2θ = 22.80° with the (130) reflection and was indexed to ICDD PDF Card No. 00-002-0534, belonging to the C2/m (No. 12) space group. Quartz was identified at 2θ = 53.19° through the (212) reflection. The

occurrence of these silicate minerals suggests the presence of naturally associated gangue phases commonly found in geological magnetite deposits. Although present in relatively small quantities, these accessory minerals may influence the physicochemical characteristics of the raw material but are not expected to significantly affect its magnetic properties or its suitability as a high-density aggregate for radiation shielding applications. The dominance of the magnetite phase indicates that the sample possesses the mineralogical characteristics required for effective attenuation of ionizing radiation due to its high iron content and crystalline stability.

3.2 FTIR Features of natural magnetite

The spectroscopic technique of FTIR is a suitable tool to characterize magnetite mineral. The analysis covers the absorption band range of 4000 - 650 cm^{-1}. The spectrum shows a broad band at 1036.2cm^{-1} corresponding to Si-O stretching vibration this indicates that the sample has impurities like silicate ion and Phosphate ion (Nandiyanto et al. 2023). Also Infrared spectra indicated the presence of the followings bands 2117.127 cm^{-1} is associated with $C \equiv C$ triple bond, the band 2117.1 $cm^{-1}$is attributed to cynade ion, thiocynate ion and related ions, also a small vibration located 2877.5 $cm^{-1}$is attributed to symmetric C-H stretching this is in agreement with previous study by Mahdavi et al. (2013), and 3690.1 cm^{-1} is associated with –OH, NH_2 (Nandiyanto et al. 2023).These peaks are not intrinsic to magnetite but reflect the adsorbed water, or organic/inorganic contaminants due to nature of our geological sample.

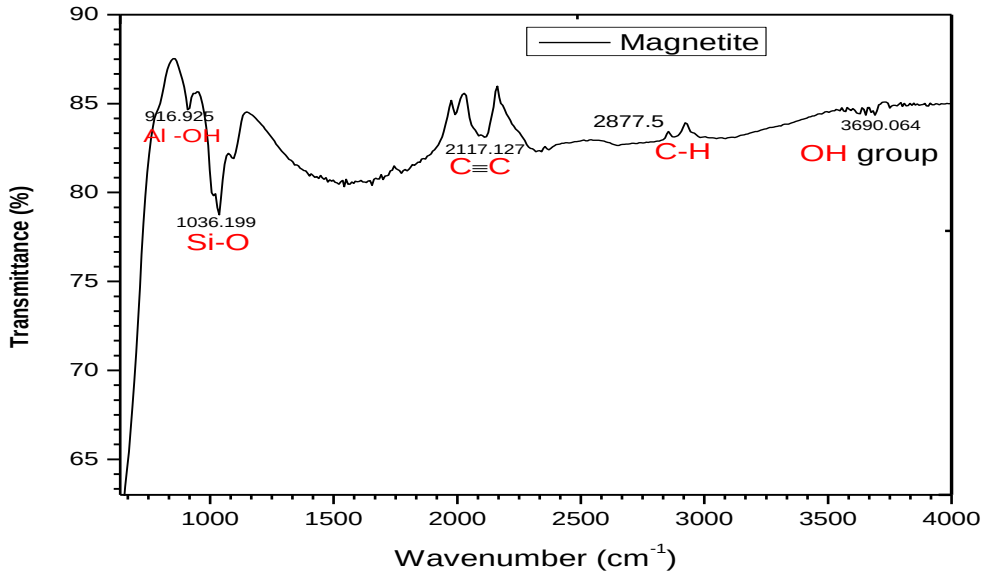

Figure 2 FTIR spectrum of magnetite mineral

3.3 Effects of Temperature on infrared spectra of natural magnetite

Fourier transform infrared (FTIR) spectroscopy was used to confirm the changes in the magnetite surface groups versus the temperature. The spectra obtained in the four heated samples of magnetite mineral compared to the unheated one in the spectral range of 600 and 4000 cm^{-1}, are shown in Figure 3. Also, figure 3 presents the FTIR spectra of the magnetite samples before and after thermal treatment at 250, 500, 750, 1000 ^{O}C. The spectra of all samples are dominated by absorption bands characteristics of hematite mineral. The analysis covers the absorption band range of 4000 - 650 cm^{-1}. For the unheated sample, the following peaks 998, 1032, and 1168 cm^{-1} are corresponding to Fe-O stretching vibrations, which serve as a clear indicator of iron o xide (Ali et al., 2016).

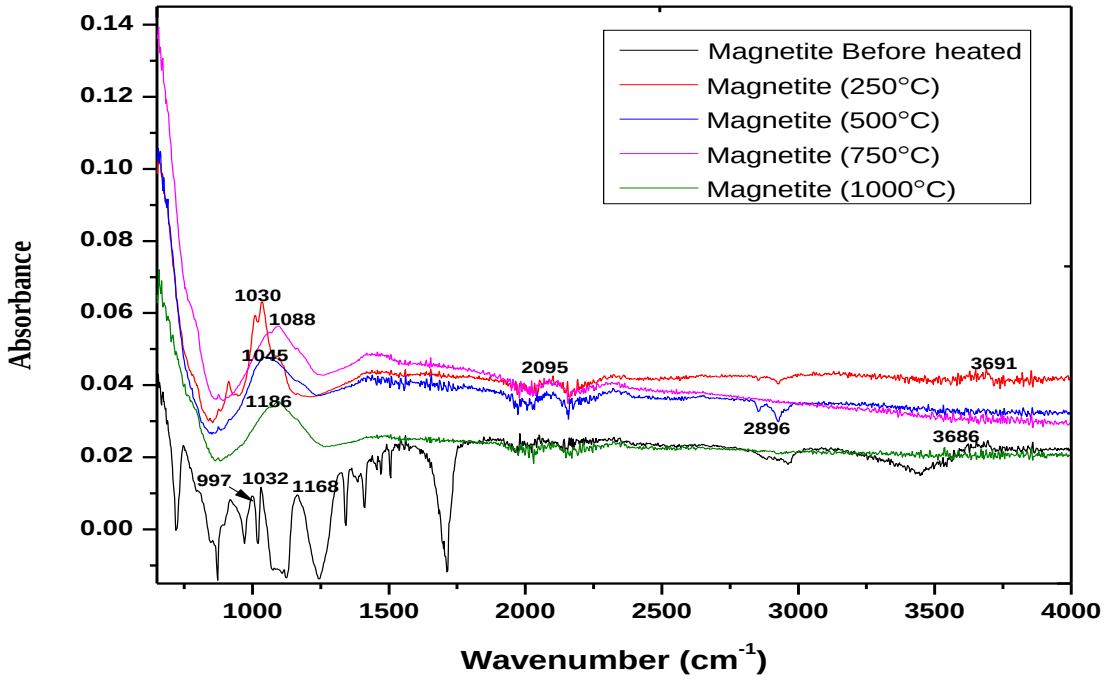

Figure 3. Infrared spectra for magnetite before heating and after heated at 250 ^{O}C, 500 ^{O}C, 750 ^{O}C and 1000^{O}C

The spectra of the samples heated at 250 °C,500 °C, 750 °C, and 1000 °C shows similar peaks pattern at 2095 cm^{-1} . Another band shifts at different temperatures were observed 1030, 1046, 1088, and 1118cm^{-1} these shift may be attributed to the structural change with temperatures in agreement with previous study (Duglet et al., 2025).This shifts of wavenumbers from higher to lower as showed in fig 3 and disappearing of 997 and 1032cm^{-1} after heated the magnetite sample indicates the change in the local bonding environment. The absorption intensity increases with the temperature these except with the sample annealed at 250 °C these increased can be attributed to the improvement of structural ordering of the magnetite mineral. Therefore, more ordered the structure is, the more this band is located at large wave numbers (Oukafir et al., 2023). Hence, the magnetite mineral is more stable at temperature below 500 °C.

3.4 TGA Analysis of magnetite mineral

Figure 4 present the TGA curve of the natural magnetite sample exhibited three distinct stages of mass loss, indicating the high thermal stability of the material with minor contributions from naturally occurring impurity phases identified by XRD, namely orthoclase and quartz.

The initial mass loss of 2.14% between 214.84 and 567.80 °C is attributed to the removal of adsorbed moisture, surface hydroxyl groups, and trace volatile impurities, while the magnetite phase remained thermally stable. A further 4.07% mass loss between 567.80 and 736.96 °C is associated with structural modifications of the silicate impurity phases, particularly orthoclase, whereas quartz remained largely stable within this temperature range.

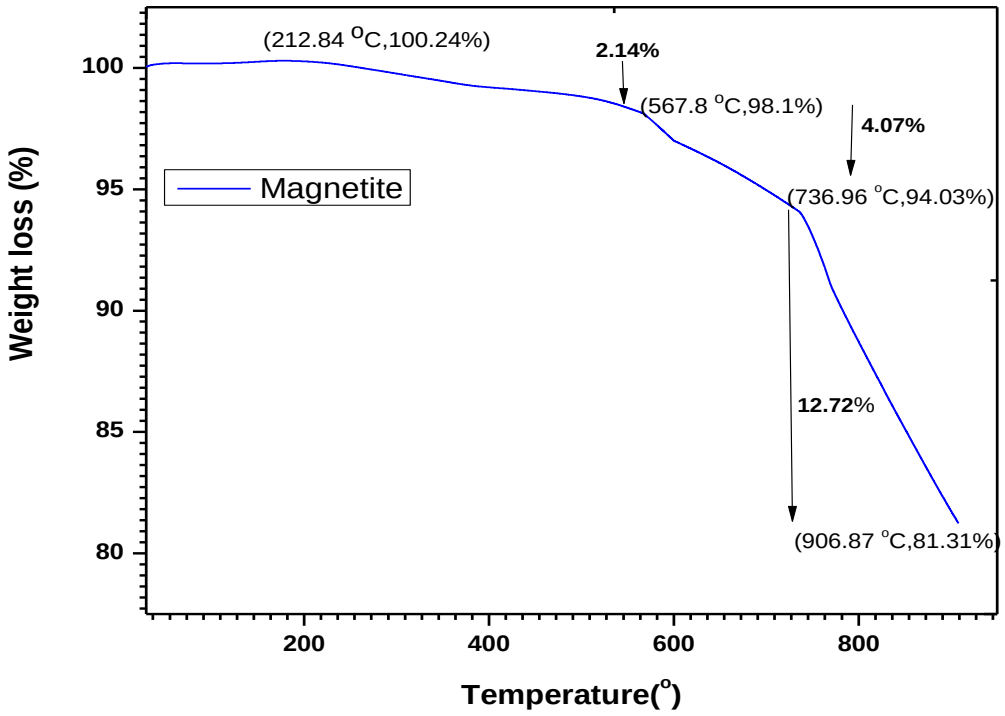

Figure 4. TGA analysis of magnetite

The highest mass loss of 12.72% occurred between 736.96 and 906.67 °C, corresponding to high-temperature mineralogical transformations under an oxidizing atmosphere. This stage is mainly attributed to the partial oxidation of magnetite (Fe_3O_4) to hematite (α-Fe_2O_3), together with structural changes in the associated gangue minerals (Monazam et al. 2014). Despite these transformations, the relatively low cumulative mass loss below approximately 500 °C confirms the excellent thermal stability of the natural magnetite. These findings

demonstrate that the material possesses adequate thermal resistance for high-temperature industrial applications, including radiation shielding concrete, refractory materials, metallurgical processes, magnetic materials, and catalyst supports, where structural integrity at elevated temperatures is essential.

4. Conclusion

This study provides a comprehensive evaluation of the structural and thermal characteristics of natural magnetite obtained from Nasarawa State, Nigeria. XRD analysis confirmed that magnetite is the dominant mineral phase, with only small amounts of quartz and orthoclase occurring as naturally associated impurities. The presence of the intense (311) diffraction peak confirmed the highly crystalline cubic spinel structure of the mineral.

The FTIR results showed that heating caused gradual changes in the vibration bands associated with the Fe–O bonds, indicating structural rearrangement as the temperature increased. However, the overall crystal framework remained largely unchanged up to about 500 °C, suggesting that the mineral retains good structural stability within this temperature range. At higher temperatures, the observed band shifts and disappearance of some absorption peaks reflected the onset of structural modifications associated with thermal treatment.

The TGA results further demonstrated the excellent thermal stability of the natural magnetite. Only minor weight loss occurred below 700 °C, while the larger mass loss observed at higher temperatures was mainly associated with oxidation of magnetite to hematite together with transformations of minor impurity minerals. These findings indicate that the studied magnetite can withstand elevated temperatures without significant degradation over a wide operating range and the stability was observed at approximately 567.8°C. Therefore, magnetite obtained from Nasarawa State is thermally stable for high-temperature technological applications such as radiation shielding concrete, refractory products, magnetic materials, catalyst supports, and other industrial systems where thermal stability is an important requirement.

Future studies should evaluate its radiation attenuation performance after thermal exposure to further establish its suitability for advanced shielding applications.

REFERENCES

Abdullah, M. A. H., Rashid, R. S. M., Amran, M., Hejazii, F., Azreen, N. M., Fediuk, R., ... & Idris, M. I. (2022). Recent trends in advanced radiation shielding concrete for construction of facilities: materials and properties. *Polymers*, *14*(14), 2830.

Abraham, A. L. B., de Ávila, M. R., Torres, R., & Diz, V. (2021). Magnetite nanoparticles as a promising non-contaminant method to control populations of fruit flies (Diptera: Tephritidae). *J. Appl. Biotechnol. Bioeng*, *8*, 112-117.

Ali, A., Zafar, H., Zia, M., ul Haq, I., Phull, A.R., Ali, J.S., et al . (2016) Synthesis, Characterization, Applications, and Challenges of Iron Oxide Nanoparticles. Nano-technology , Science and Applications , 9, 49-67.

Arakaki, A., Nakazawa, H., Nemoto, M., Mori, T., & Matsunaga, T. (2008). Formation of magnetite by bacteria and its application. *Journal of the Royal Society interface*, *5*(26), 977-999.

Bashter, I. I. (1997). Calculation of radiation attenuation coefficients for shielding concretes. Annals of Nuclear Energy, 24(17), 1389–1401.

Bustamante-Torres, M., Romero-Fierro, D., Estrella-Nuñez, J., Arcentales-Vera, B., Chichande-Proaño, E., & Bucio, E. (2022). Polymeric composite of magnetite iron oxide nanoparticles and their application in biomedicine: a review. *Polymers*, *14*(4), 752.

Cornell, R. M., & Schwertmann, U. (2003). The Iron Oxides: Structure, Properties, Reactions, Occurrences and Uses (2nd ed.). Wiley-VCH.

Dudchenko, N., Pawar, S., Perelshtein, I., & Fixler, D. (2022). Magnetite nanoparticles: Synthesis and applications in optics and nanophotonics. *Materials*, *15*(7), 2601.

Duglet, A., et al. (2025). Thermal evolution and structural behavior of iron oxide minerals under elevated temperatures. Journal of Thermal Analysis and Calorimetry. (Update with complete bibliographic details before submission.)

Duglet, R., Sharma,D., Singh,V, Sharma, D., &Singh,M.(2025).Temperature-driven evolution of hematite (α-Fe_2O_3) nanoparticles: A study on structural, morphological and magnetic properties. Solid State Communications,396, 115761

Fawcett, T., et al. (2022). The Powder Diffraction File (PDF®): Past, present and future. Powder Diffraction, 37(S1), S1–S8.

Fock, J., Bogart, L. K., González-Alonso, D., Espeso, J. I., Hansen, M. F., Varón, M., ... & Pankhurst, Q. A. (2017). On the 'centre of gravity'method for measuring the composition of magnetite/maghemite mixtures, or the stoichiometry of magnetite-maghemite solid solutions, via 57Fe Mössbauer spectroscopy. *Journal of Physics D: Applied Physics*, *50*(26), 265005.

He, J., Li, K., Zhang, J., & Conejo, A. N. (2023). Reduction kinetics of compact hematite with hydrogen from 600 to 1050 C. *Metals*, *13*(3), 464.

Jeong, S., Jeong, H., Yang, S. J., Cho, S., & Chung, H. (2024). Intelligent color image analysis of sintered ores for simple and rapid determination of Fe3O4 concentration. *Talanta*, *274*, 125985.

Khan, S. A., Khan, S. B., Khan, L. U., Farooq, A., Akhtar, K., & Asiri, A. M. (2018). Fourier transform infrared spectroscopy: fundamentals and application in functional groups and nanomaterials characterization. *Handbook of materials characterization*, 317-344.

Liu, M., Ye, Y., Ye, J., Gao, T., Wang, D., Chen, G., & Song, Z. (2023). Recent advances of magnetite (Fe3O4)-based magnetic materials in catalytic applications. *Magnetochemistry*, *9*(4), 110.

Mahdavi, M., Ahmad M.B, Haron M., J, Namvar, F., Nadi, B, Rahman M., Z & Amin,J.(2013). Synthesis, Surface Modification and Characterisation of Biocompatible Magnetic Iron Oxide Nanoparticles for Biomedical Applications.*Molecules, 18,* 7533-7548; doi:10.3390/molecules18077533.

Morel, A. L., et al. (2013). Sonochemical approach to the synthesis of Fe_3O_4 nanoparticles. Journal of Nanomaterials, 2013, Article ID 920915.

Monazam, E.R., Breault, R.W.,& Siriwardane, R. (2014).Kinetic of Magnetite(Fe3O4) Oxidation to Hematite (Fe2O3) in Air for chemical looping combustion. Industrial &Engineering Chemistry Research, 53(31),12231-12239.

Murbe, J., et al. (2008). Structural characterization of magnetite using X-ray diffraction and complementary techniques. Crystal Research and Technology, 43(9), 1027–1033.

Namduri, H., Nasrazadani, S., & Schumaker, P. (2014). Quantitative analysis of iron oxides using Fourier transforms infrared spectrophotometry, corrosion Scienece, 79, 1-8.

Nandiyanto, A. B. D., Ragadhita, R., & Fiandini, M. (2023). Interpretation of Fourier Transform Infrared Spectra (FTIR): A Practical Approach in the Polymer/Plastic Thermal Decomposition, *Indonesian Journal of Science & Technology* 8(1) 113-126DOI: https://doi.org/10.17509/ijost.v8i1.53297

Oufakir, A. and Khouchaf, L. (2023) Structural and Surface Changes of SiO2 Flint Aggregates under Thermal Treatment for Potential Valorization. Crystals, 13, 647. https://doi.org/10.3390/cryst13040647

Reddy, A. L. S. B., Sahoo, S. K., & Kumar, M. (2023). Studies on characterization of properties of low-grade hematite iron ores and their fired pellets. *Ironmaking & Steelmaking*, *50*(9), 1215-1223.

Santillo, C.,Piochi, M.,De Vivo,B.,&Somma,R. (2015).Raman and FTIR spectroscopy of iron oxides in volcanic environments: Implications of mineral identification and phase transformation studies. Journal of Molecular Structure, 1099, 94-10

Singh, V. P., et al. (2018). Radiation shielding properties of heavy-weight concrete containing magnetite aggregates. Construction and Building Materials, 191, 1044–1055.